Leaky Dispersion Characteristics in Circular Dielectric Rod Using Davidenko's Method

Ki Young Kim[1] · Heung-Sik Tae[1] · Jeong-Hae Lee[2]

Abstract

The leaky dispersion characteristics of a circular dielectric rod were investigated using Davidenko's method for several lower-order transverse magnetic(TM) modes. The normalized complex propagation constants were precisely determined and their tolerances below 10^{-10} compared with zero for both real and imaginary parts. It was also checked whether the normalized complex propagation constants obtained represented forward leaky waves. The leaky modes existing below the cutoff frequency of the guided mode were classified as a nonphysical mode, reactive mode, antenna mode, and spectral gap based on a precise determination of the complex propagation constants. Finally, the effects of the dielectric constant and radius of the dielectric rod on the leaky dispersion characteristics were also considered.

Key words : Circular Dielectric Rod, Davidenko's Method, Leaky Mode, Normalized Phase Constants, Normalized Attenuation Constants.

Ⅰ. Introduction

Since a circular dielectric rod is one of the simplest guiding structures, its guided mode characteristics have already been studied for a long time[1]. However, the leaky mode characteristics of a circular dielectric rod are not well known, even though the leaky modes for various partially open waveguides are relatively well analyzed, especially for printed circuit lines(for example, ref. [2] and the references therein). In 1969, Arnbak[3] demonstrated the existence of leaky modes in a circular dielectric rod using an approximation of the characteristic equation. Yet, no further research results on the leaky modes of a circular dielectric rod have been reported, even though this structure has significant potential as a simple, low loss, and low cost omnidirectional leaky wave antenna. In leaky modes, the propagation constant in the propagating direction is complex. The imaginary part of the complex propagation constant is not derived from the absorption by the medium, but rather from the leakage of the propagating power into free space. The phase and attenuation constants in the complex propagation constant are two of the most important and fundamental parameters in analyzing leaky waves. Therefore, since the complex propagation constant can reveal insights on leaky waves, it is quite important to determine the exact complex propagation constants prior to the analysis of leaky modes. Several previous publications have included information on obtaining the complex roots of complex functions using Davidenko's method[4]~[10]. Due to its insensitivity to initial guesses and high speed of convergence, Davidenko's method is known to be superior over other conventional complex root search algorithms, such as Newton-Raphson's method or Müller's method[11], plus Davidenko's method can find solutions, even when other methods fail to converge[4]. Accordingly, Davidenko's method has already been used to solve the dispersion equation of a cylindrical substrate-superstrate layered medium[5] and obtain the complex zeros of the Hankel's functions in the order plane[6]. Furthermore, Davidenko's method has also been used to obtain the complex propagation constants in various guiding structures, such as lossy waveguides including gyrotropic layers[7], surface plasmon polaritons[8], moving optical waveguides[9], and lossy nonlinear waveguides[10]. As such, these successful applications demonstrate that Davidenko's method is currently the most effective method for determining the complex propagation constants of leaky waves in a circular dielectric rod.

Accordingly, the current paper uses Davidenko's method to determine the complex propagation constants of the complex characteristic equation of a circular dielectric rod. No modification to the characteristic equation of a circular dielectric rod is required for the application of Davidenko's method. Thus, the leaky dispersion characteristics of a circular dielectric rod are

Manuscript received March 29, 2005 ; revised May 25, 2005. (ID No. 20050329-008J)

[1]School of Electrical Engineering and Computer Science, Kyungpook National University, Daegu, Korea.
[2]Department of Radio Science and Communication Engineering, Hongik University, Seoul, Korea.

analyzed for several lower-order *TM* modes based on precisely determined complex propagation constants. Various modes are investigated, including the non-physical mode, antenna mode, reactive mode, and spectral gap, all of which exist within leaky modes. The effects of two design parameters, the dielectric constant and radius of the rod, on the leaky dispersion characteristics are also examined.

II. Characteristic Equation

Fig. 1 shows the schematic geometry of the circular dielectric rod employed in the current research, where a is the radius of the rod, which is surrounded by free space, ε_{r1} and ε_{r2} are the dielectric constants of the dielectric medium and surrounding free-space medium, respectively, and μ_{r1} and μ_{r2} are the relative permeability in each region, respectively. In the current study, ε_{r2}, μ_{r1}, and μ_{r2} are assumed to be unity. Since the hybrid mode is the linear combination of the *TM* and *TE* modes, and the two transverse modes are identical except for their material constants, the TM_{0n} mode exhibits the most general feature of the circular dielectric rod and is the main focus of the current study. The characteristic equation of the circular dielectric rod for the TM_{0n} mode can be given in the following form [12].

$$Q=\frac{\varepsilon_{r1}}{k_1}\frac{J_1(k_1a)}{J_0(k_1a)}-\frac{\varepsilon_{r2}}{k_2}\frac{H_1^{(2)}(k_2a)}{H_0^{(2)}(k_2a)}=0. \tag{1}$$

Here, $J_m(\cdot)$ and $H_m^{(2)}(\cdot)$ $(m=0, 1)$ are the mth order Bessel function and the Hankel function of the second kind, respectively, and k_1 and k_2 are the complex transverse propagation constants of the dielectric region and free space region, respectively, which are related with the normalized complex axial propagation constant $\bar{\gamma}$,

$$k_i^2=k_0^2\mu_{ri}\varepsilon_{ri}-\gamma^2=k_0^2\left(\mu_{ri}\varepsilon_{ri}-\bar{\gamma}^2\right)\quad (i=1,2) \tag{2}$$

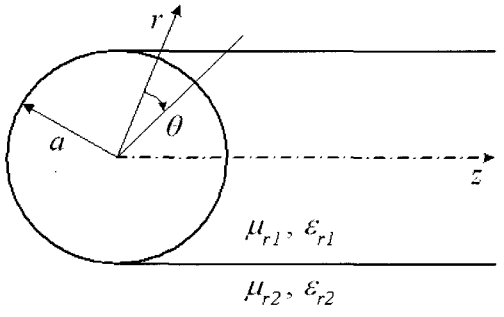

Fig. 1. Schematic diagram of circular dielectric rod surrounded by free space.

where k_0 is the free space wavenumber. The normalized complex axial propagation constant $\bar{\gamma}$ can be defined as follows:

$$\bar{\gamma}=\frac{\gamma}{k_0}=\frac{\beta-j\alpha}{k_0}=\frac{\beta}{k_0}-j\frac{\alpha}{k_0}=\bar{\beta}-j\bar{\alpha} \tag{3}$$

where $\bar{\beta}$ and $\bar{\alpha}$ are the normalized phase and attenuation constants, respectively.

If the complex transverse propagation constant is $k_i=\mathrm{Re}\{k_i\}+j\mathrm{Im}\{k_i\}$, $(i=1, 2)$ the normalized complex transverse propagation constants, as in the case of axial ones, can be defined as follows:

$$\bar{k}_i=\frac{k_i}{k_0}=\frac{\mathrm{Re}\{k_i\}+j\,\mathrm{Im}\{k_i\}}{k_0}=\frac{\mathrm{Re}\{k_i\}}{k_0}+j\frac{\mathrm{Im}\{k_i\}}{k_0}$$
$$=\mathrm{Re}\left\{\frac{k_i}{k_0}\right\}+j\,\mathrm{Im}\left\{\frac{k_i}{k_0}\right\}=\mathrm{Re}\left\{\bar{k}_i\right\}+j\,\mathrm{Im}\left\{\bar{k}_i\right\} \tag{4}$$

and the following relationships should be satisfied from Eqs. (2), (3), and (4)[13].

$$\begin{cases}\left(\mathrm{Re}\left\{\bar{k}_i\right\}\right)^2-\left(\mathrm{Im}\left\{\bar{k}_i\right\}\right)^2=\mu_{ri}\varepsilon_{ri}-\bar{\beta}^2+\bar{\alpha}^2\\ \mathrm{Re}\left\{\bar{k}_i\right\}\mathrm{Im}\left\{\bar{k}_i\right\}=\bar{\alpha}\bar{\beta}\end{cases} \tag{5}$$

Eq. (5) is the condition for general complex waves. In addition to Eq. (5), the conditions for forward leaky waves are $\bar{\beta}>0$, $\bar{\alpha}>0$, $\mathrm{Re}\{\bar{k}_i\}>0$, and $\mathrm{Im}\{\bar{k}_i\}>0$[13].

III. Davidenko's Method

Davidenko's method was used to determine the complex root(here, the normalized complex axial propagation constants, *i.e.*, $\bar{\beta}$ and $\bar{\alpha}$) satisfying the characteristic equation (1). If the dielectric constants of each region, radius of the dielectric rod, and operating frequency are given, the characteristic equation for the TM_{0n} mode, Eq. (1), can be expressed by a function of the normalized phase and attenuation constants, *i.e.*, $Q(\bar{\beta}, \bar{\alpha})=0$ or $Q(\bar{\gamma})=0$.

In principle, Davidenko's method transforms n-coupled nonlinear algebraic equations into an n-coupled first-order differential equation with an independent scalar dummy variable[4]~[10]. For $n=2$, *i.e.*, two variables, here $\bar{\beta}$ and $\bar{\alpha}$, we can start from the following equation:

$$\frac{d\bar{\gamma}}{dt}=-J^{-1}Q\left(\bar{\gamma}\right) \tag{6}$$

where t is a scalar dummy variable which is independent of $\bar{\gamma}$ $(=\bar{\beta}+j\bar{\alpha})$[1]. The normalized complex propagation constant $\bar{\gamma}$ and the complex characteristic equation

$Q(\bar{\gamma})$ can also be expressed as the following column vectors, respectively.

$$\bar{\gamma} = \begin{bmatrix} \bar{\beta} \\ \bar{\alpha} \end{bmatrix} \tag{7}$$

$$Q(\bar{\gamma}) = \begin{bmatrix} \mathrm{Re}\{Q(\bar{\gamma})\} \\ \mathrm{Im}\{Q(\bar{\gamma})\} \end{bmatrix} \tag{8}$$

Substituting Eqs. (7) and (8) into Eq. (6), we can rewrite Eq. (6) as follows:

$$\frac{d}{dt}\begin{bmatrix} \bar{\beta} \\ \bar{\alpha} \end{bmatrix} = -J^{-1}\begin{bmatrix} \mathrm{Re}\{Q(\bar{\gamma})\} \\ \mathrm{Im}\{Q(\bar{\gamma})\} \end{bmatrix}. \tag{9}$$

J is a Jacobian matrix of the following form:

$$J = \begin{bmatrix} \mathrm{Re}\left\{\frac{\partial Q(\bar{\gamma})}{\partial \bar{\beta}}\right\} & \mathrm{Re}\left\{\frac{\partial Q(\bar{\gamma})}{\partial \bar{\alpha}}\right\} \\ \mathrm{Im}\left\{\frac{\partial Q(\bar{\gamma})}{\partial \bar{\beta}}\right\} & \mathrm{Im}\left\{\frac{\partial Q(\bar{\gamma})}{\partial \bar{\alpha}}\right\} \end{bmatrix} \tag{10}$$

While, using the Cauchy-Riemann relation[14], total derivative of $Q(\bar{\gamma})$ with respect to $\bar{\gamma}$, *i.e.*, $Q_{\bar{\gamma}}(\bar{\gamma})$, can be expressed as follows due to the analyticity of $Q(\bar{\gamma})$.

$$\begin{aligned} Q_{\bar{\gamma}}(\bar{\gamma}) &= \frac{dQ(\bar{\gamma})}{d\bar{\gamma}} \qquad \bar{\gamma} = \bar{\beta} - j\bar{\alpha} \\ &= \mathrm{Re}\left\{\frac{\partial Q(\bar{\gamma})}{\partial \bar{\beta}}\right\} + j\,\mathrm{Im}\left\{\frac{\partial Q(\bar{\gamma})}{\partial \bar{\beta}}\right\} \\ &= \mathrm{Re}\left\{\frac{\partial Q(\bar{\gamma})}{\partial \bar{\beta}}\right\} - j\,\mathrm{Re}\left\{\frac{\partial Q(\bar{\gamma})}{\partial \bar{\alpha}}\right\} \end{aligned} \tag{11}$$

Thus, the real and imaginary terms of $Q_{\bar{\gamma}}(\bar{\gamma})$ are given as follows.

$$\begin{cases} \mathrm{Re}\{Q_{\bar{\gamma}}(\bar{\gamma})\} = \mathrm{Re}\left\{\frac{\partial Q(\bar{\gamma})}{\partial \bar{\beta}}\right\} \\ \mathrm{Im}\{Q_{\bar{\gamma}}(\bar{\gamma})\} = -\mathrm{Re}\left\{\frac{\partial Q(\bar{\gamma})}{\partial \bar{\alpha}}\right\} \end{cases} \tag{12}$$

Using the Cauchy-Riemann relation again, *i.e.*, $\mathrm{Re}\{\partial Q(\bar{\gamma})/\partial\bar{\beta}\} = \mathrm{Im}\{\partial Q(\bar{\gamma})/\partial\bar{\alpha}\}$ and $\mathrm{Re}\{\partial Q(\bar{\gamma})/\partial\bar{\alpha}\} = -\mathrm{Im}\{\partial Q(\bar{\gamma})/\partial\bar{\beta}\}$, the above Jacobian matrix in (10) can be rewritten as follows.

$$J = \begin{bmatrix} \mathrm{Re}\left\{\frac{\partial Q(\bar{\gamma})}{\partial \bar{\beta}}\right\} & \mathrm{Re}\left\{\frac{\partial Q(\bar{\gamma})}{\partial \bar{\alpha}}\right\} \\ -\mathrm{Re}\left\{\frac{\partial Q(\bar{\gamma})}{\partial \bar{\alpha}}\right\} & \mathrm{Re}\left\{\frac{\partial Q(\bar{\gamma})}{\partial \bar{\beta}}\right\} \end{bmatrix} \tag{13}$$

Then, the Jacobian matrix of (13) can be expressed using the relations in (12) as follows:

$$J = \begin{bmatrix} \mathrm{Re}\{Q_{\bar{\gamma}}(\bar{\gamma})\} & -\mathrm{Im}\{Q_{\bar{\gamma}}(\bar{\gamma})\} \\ \mathrm{Im}\{Q_{\bar{\gamma}}(\bar{\gamma})\} & \mathrm{Re}\{Q_{\bar{\gamma}}(\bar{\gamma})\} \end{bmatrix} \tag{14}$$

and the inverse form the Jacobian matrix in (14) can be written as follows:

$$J^{-1} = -\frac{1}{\det J}\begin{bmatrix} \mathrm{Re}\{Q_{\bar{\gamma}}(\bar{\gamma})\} & \mathrm{Im}\{Q_{\bar{\gamma}}(\bar{\gamma})\} \\ -\mathrm{Im}\{Q_{\bar{\gamma}}(\bar{\gamma})\} & \mathrm{Re}\{Q_{\bar{\gamma}}(\bar{\gamma})\} \end{bmatrix} \tag{15}$$

where

$$\det J = \left[\mathrm{Re}\{Q_{\bar{\gamma}}(\bar{\gamma})\}\right]^2 + \left[\mathrm{Im}\{Q_{\bar{\gamma}}(\bar{\gamma})\}\right]^2 = \left|Q_{\bar{\gamma}}(\bar{\gamma})\right|^2. \tag{16}$$

Therefore, Eq. (6) can be expressed in a matrix form as follows:

$$\begin{aligned} \frac{d}{dt}\begin{bmatrix} \bar{\beta} \\ \bar{\alpha} \end{bmatrix} = -\frac{1}{\left|Q_{\bar{\gamma}}(\bar{\gamma})\right|^2}&\begin{bmatrix} \mathrm{Re}\{Q_{\bar{\gamma}}(\bar{\gamma})\} & \mathrm{Im}\{Q_{\bar{\gamma}}(\bar{\gamma})\} \\ -\mathrm{Im}\{Q_{\bar{\gamma}}(\bar{\gamma})\} & \mathrm{Re}\{Q_{\bar{\gamma}}(\bar{\gamma})\} \end{bmatrix} \\ &\times\begin{bmatrix} \mathrm{Re}\{Q(\bar{\gamma})\} \\ \mathrm{Im}\{Q(\bar{\gamma})\} \end{bmatrix} \end{aligned} \tag{17}$$

Finally, two coupled first-order ordinary differential equations with two unknowns, $\bar{\beta}$ and $\bar{\alpha}$, from Eq. (1) using Davidenko's algorithm can be written as follows.

$$\begin{cases} \frac{d\bar{\beta}}{dt} = -\frac{\mathrm{Re}[Q(\bar{\gamma})]\mathrm{Re}[Q_{\bar{\gamma}}(\bar{\gamma})] + \mathrm{Im}[Q(\bar{\gamma})]\mathrm{Im}[Q_{\bar{\gamma}}(\bar{\gamma})]}{\left|Q_{\bar{\gamma}}(\bar{\gamma})\right|^2} \\ \frac{d\bar{\alpha}}{dt} = \frac{\mathrm{Re}[Q(\bar{\gamma})]\mathrm{Im}[Q_{\bar{\gamma}}(\bar{\gamma})] - \mathrm{Im}[Q(\bar{\gamma})]\mathrm{Re}[Q_{\bar{\gamma}}(\bar{\gamma})]}{\left|Q_{\bar{\gamma}}(\bar{\gamma})\right|^2} \end{cases} \tag{18}$$

Eq. (18) is solved for a large t using the software package MATHEMATICA 4.0(utilizing **NDSolve** and **InterpolatingFunction**, internal functions of the MATHEMATICA package)[15]. The resulting normalized phase and attenuation constants are then substituted into the original TM_{0n} mode characteristic function $Q(\bar{\gamma})$. The tolerances of the ensuing values are checked by comparing them with the zeros for both the real and imaginary parts. For the procedure of solving Eq. (18), when t is set larger, the tolerance can have a smaller value, yet it takes longer to converge, therefore, the tolerance was arbitrarily set at 10^{-10} for both the real parts and the imaginary parts. The obtained roots also satisfy the set of Eq. (5) and represent forward leaky waves, that is $\bar{\beta}>0$, $\bar{\alpha}>0$, $\mathrm{Re}\{\bar{k}_i\}>0$, and $\mathrm{Im}\{\bar{k}_i\}>0$ as

[1] In this section, $\bar{\gamma} = \bar{\beta} + j\bar{\alpha}$ is used instead of $\bar{\gamma} = \bar{\beta} - j\bar{\alpha}$ in Eq. (3) for simplicity in applying Davidenko's method. From the calculated resulting values, we changed the sign of $\bar{\alpha}$. The numerical results will be shown in the next section.

mentioned in the previous section.

Ⅳ. Numerical Results and Discussion

Fig. 2(a) and (b) show the normalized phase and attenuation constants for four lower-order TM_{0n} modes, respectively, with variations in the operating frequency ranging from 0 to 60 GHz. The dielectric constant and radius of the rod were arbitrarily selected to be 5.0 and 5.0 mm, respectively. As shown in Fig. 2(a) and (b), as the frequency approached zero, the normalized phase and attenuation constants grew rapidly. In spite of a different guiding structure, this property is well described in [16]. However, the normalized phase constant in the frequency region ranging from 0 to 3.51 GHz, where the normalized phase constant exceeded unity, was physically meaningless[16]. Yet, as the modes became higher, the upper limit frequencies of this nonphysical frequency region shifted toward lower frequencies, as shown in Fig. 2(a). More detailed numerical data are listed in Table 1. In the frequency region higher than the nonphysical frequency region, the normalized phase constants decreased to certain minimum points and then increased again to unity, as seen in Fig. 2(a). This frequency region, in which the normalized phase constant was physically meaningful, was divided into two distinct regions; a reactive mode region ($\bar{\beta}<1$ and $\bar{\beta}<\bar{\alpha}$) where the guided imaginary power was larger than the guided real power, and an antenna mode region($\bar{\beta}<1$ and $\bar{\beta}<\bar{\alpha}$).

Where the guided real power was larger than the guided imaginary power[17]. As shown in Fig. 2(a) and Table 1, the spectral widths of both the reactive and antenna mode regions increased as the modes became higher, except for the TM_{01} mode. However, it should be noted that the TM_{01} mode ranging from 3.51 to 11.48 GHz was not separated into two regions in the case of the dielectric rod employed in the current research. In other words, only an antenna mode region was observed in the TM_{01} mode, since the normalized phase

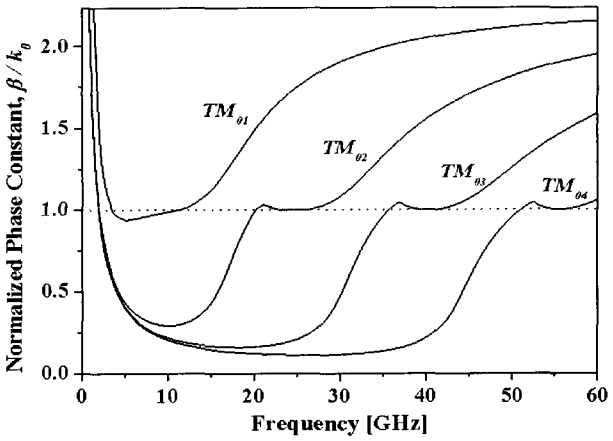

(a)

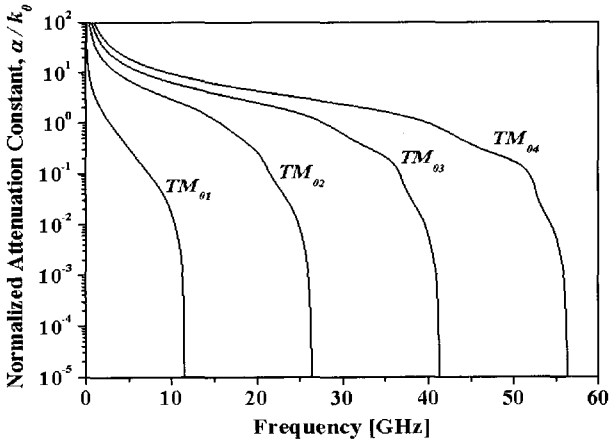

(b)

Fig. 2. (a) Normalized phase constants and (b) normalized attenuation constants when dielectric constant and radius of dielectric rod are 5.0 and 5.0 mm, respectively.

constant was always greater than the normalized attenuation constant in the physically meaningful frequency region. As the frequency became higher beyond the first antenna mode region, the normalized phase constants exceeded unity again. Fig. 3 shows an enlarged scale of the normalized phase constants in the vicinity of unity.

Table 1. Spectral ranges of various modes in leaky modes for cases of ε_{r1}=5.0 and a=5.0 mm(Spectral widths).

Mode	Nonphysical mode	Reactive mode	1st Antenna mode	Spectral gap	2nd Antenna mode	Guided mode cutoff
TM_{01}	0~3.51 GHz (3.51 GHz)	Not available	Not available	Not available	3.51~11.48 GHz (7.97 GHz)	11.48 GHz
TM_{02}	0~1.98 GHz (1.98 GHz)	1.98~17.15 GHz (15.17 GHz)	17.15~20.27 GHz (3.12 GHz)	20.27~22.84 GHz (2.57 GHz)	22.84~26.35 GHz (3.51 GHz)	26.35 GHz
TM_{03}	0~1.95 GHz (1.95 GHz)	1.95~30.57 GHz (28.62 GHz)	30.57~35.76 GHz (5.19 GHz)	35.76~39.13 GHz (3.37 GHz)	39.13~41.31 GHz (2.18 GHz)	41.31 GHz
TM_{04}	0~1.94 GHz (1.94 GHz)	1.94~43.93 GHz (41.99 GHz)	43.93~51.17 GHz (7.24 GHz)	51.17~54.70 GHz (3.53 GHz)	54.70~56.30 GHz (1.60 GHz)	56.30 GHz

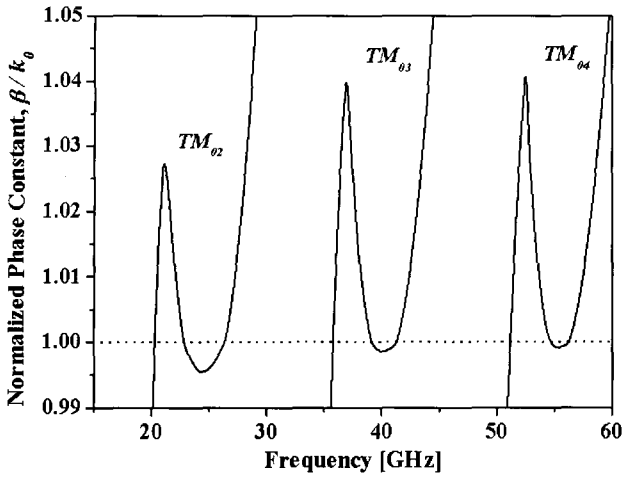

Fig. 3. Enlarged scale of normalized phase constants near unity.

The narrow spectral ranges of the normalized phase constants greater than unity, as shown in Fig. 3, are called spectral gaps[18]. A spectral gap is physically meaningless, as is a nonphysical frequency region. The TM_{01} mode does not have a spectral gap, which is generally defined as the transition region from the leaky mode($\bar{\alpha}>0$) into the guided mode($\bar{\alpha}=0$). However, in the current study, it was found that the nonzero value of the normalized attenuation constants remained for the whole spectral gap, as shown in Figs. 2(b) and 3, indicating that the spectral gap is not always consistent with the transition region between the leaky and guided modes. As shown in Fig. 3, the width of the spectral gap increased as the modes became higher. In the frequency region above the spectral gap, there was another antenna mode, *i.e.*, second antenna mode region, where the normalized phase constants became less than unity, as shown in Fig. 3. The spectral width of the second antenna mode decreased as the modes became higher. As for the TM_{01} mode, there was only one antenna mode. However, based on the tendency of the spectral widths of the other antenna modes(*i.e.*, the spectral widths of the first antenna modes increased with a higher-order mode, whereas the spectral widths of the second antenna modes decreased with a higher-order mode, as shown in Table 1), the antenna mode for the TM_{01} mode was categorized as a second antenna mode. The upper limit of the second antenna mode region met the cutoff frequency of the guided mode, after which the propagation constants became real.

Fig. 4(a) and (b) show the real and imaginary parts of the normalized complex transverse propagation constants in each region for the TM_{01} and TM_{02} modes, respectively, in the leaky mode region, *i.e.*, below the cutoff frequency of the guided mode region. In that

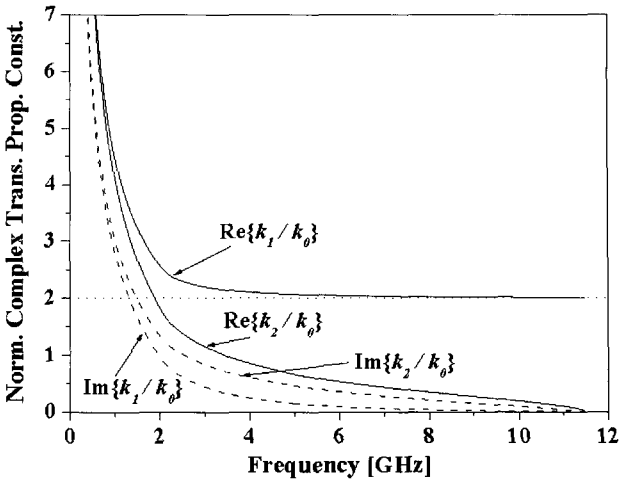

(a)

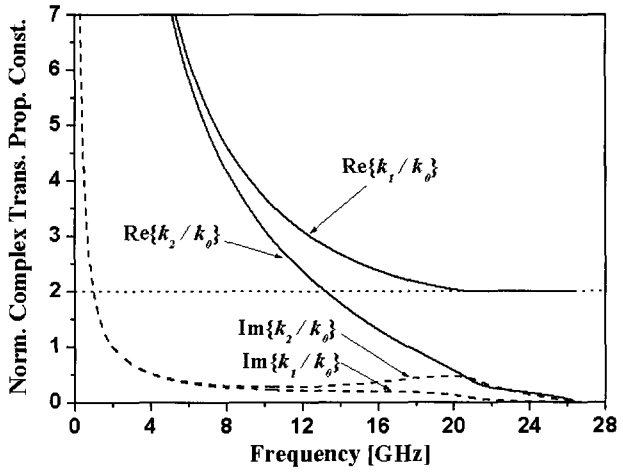

(b)

Fig. 4. Normalized complex transverse propagation constants. (a) TM_{01} mode and (b) TM_{02} mode.

region, the real and imaginary parts of the normalized complex transverse propagation constants were all positive, meaning that the solution represented forward leaky waves, as mentioned in the previous two sections. As the operating frequency reached the cutoff frequency of the guided mode, the real part of the normalized complex transverse propagation constant in the dielectric region approached $2(=\sqrt{\mu_{r1}\varepsilon_{r1}-1})$, while the others became zero, as shown in Figs. 4(a) and (b). As such, the propagation constant in the free space region at the cutoff frequency became unity from eq. (2), which was the same as the free space propagation constant. Accordingly, at this cutoff frequency, the electromagnetic fields were no longer confined to the dielectric region. Above this cutoff frequency, the normalized propagation (phase) constant for the rod became real and higher than unity, thereby supporting the guided mode with evanescent waves in the free-space region.

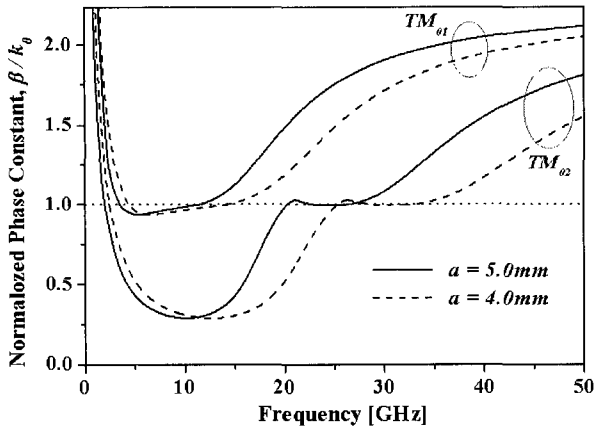

Fig. 5. Normalized phase constants of first two *TM* modes when dielectric constant of dielectric rod is 5.0 with different radii(a=5.0 mm and a= 4.0 mm).

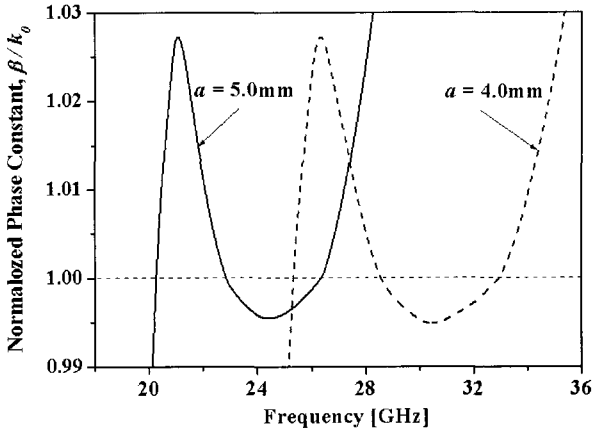

Fig. 6. Enlarged scale of normalized phase constants near unity for TM_{02} mode when dielectric constant of dielectric rod is 5.0 with different radii(a=5.0 mm and a=4.0 mm).

Next, the effects of two design parameters, the dielectric constant and radius of the rod, on the leaky dispersion characteristics were briefly considered. Fig. 5 shows the normalized phase constants of the first two *TM* modes with different rod radii(a=5.0 mm and a=4.0 mm). The tendency in the dispersion curve in Fig. 5 shows that the normalized phase constant curves for both the TM_{01} and TM_{02} modes shifted toward a higher frequency regime with a decrease in the radius of the rod. An enlarged scale of the normalized phase constant near unity for the TM_{02} mode is shown in Fig. 6. Since there was no spectral gap in the case of the TM_{01} mode, only the TM_{02} mode case is shown in Fig. 6. The detailed leaky characteristics of the TM_{01} and TM_{02} modes relative to the radius of the rod are listed in Table 2(a), where the spectral widths of the nonphysical frequency regions, reactive mode regions, two antenna mode regions, and spectral gap regions tended to increase with a decrease in the radius of the rod for the TM_{01} and TM_{02} modes.

With different rod dielectric constants(ε_{r1}=5.0 and ε_{r1} =4.0), the normalized phase constants of the first two *TM* modes varied with the operating frequency, as shown in Fig. 7. The effect of the rod dielectric constant on the dispersion characteristics of the normalized phase constant exhibited the same tendency as that of the rod radius, as shown in Fig. 7. As for the TM_{02} mode, an enlarged scale near unity is also shown in Fig. 8.

The detailed leaky characteristics of the TM_{01} and TM_{02} modes relative to the rod dielectric constant are listed in Table 2(b), where the spectral widths of the nonphysical mode regions, reactive mode regions, first antenna mode regions, and spectral gap regions all increased with a decrease in the rod dielectric constant.

Table 2. Changes in spectral widths (a) Spectral widths with same dielectric constant(ε_{r1}=5.0) and different radii (a=5.0 mm and a=4.0 mm). (b) Spectral widths with same radius(a=5.0 mm) and different dielectric constants(ε_{r1}=5.0 and ε_{r1}=4.0).

(a)						
Mode	Radii	Nonphysical mode	Reactive mode	1st Antenna mode	Spectral gap	2nd Antenna mode
TM_{01}	5.0 mm 4.0 mm	3.51 GHz 4.39 GHz	Not available	Not available	Not available	7.97 GHz 9.97 GHz
TM_{02}	5.0 mm 4.0 mm	1.98 GHz 2.47 GHz	15.17 GHz 18.96 GHz	3.12 GHz 3.91 GHz	2.57 GHz 3.21 GHz	3.51 GHz 4.40 GHz
(b)						
Mode	Dielectric constant	Nonphysical mode	Reactive mode	1st Antenna mode	Spectral gap	2nd Antenna mode
TM_{01}	5.0 4.0	3.51 GHz 4.61 GHz	Not available	Not available	Not available	7.97 GHz 8.65 GHz
TM_{02}	5.0 4.0	1.98 GHz 2.50 GHz	15.17 GHz 16.69 GHz	3.12 GHz 4.56 GHz	2.57 GHz 3.26 GHz	3.51 GHz 3.42 GHz

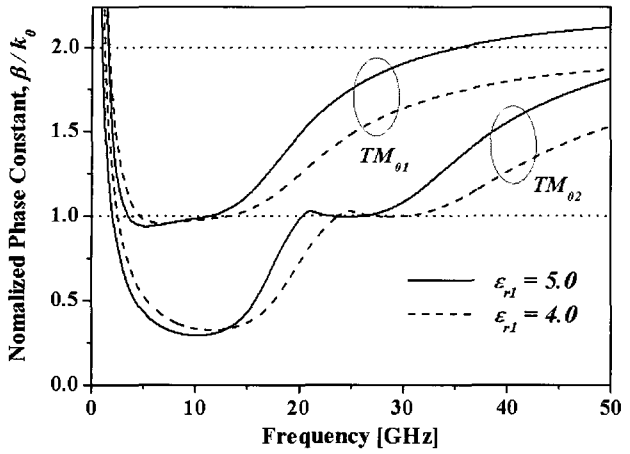

Fig. 7. Normalized phase constants of first two TM modes when radius of dielectric rod is 5.0 mm with different dielectric constants(ε_{r1}=5.0 and ε_{r1} =4.0).

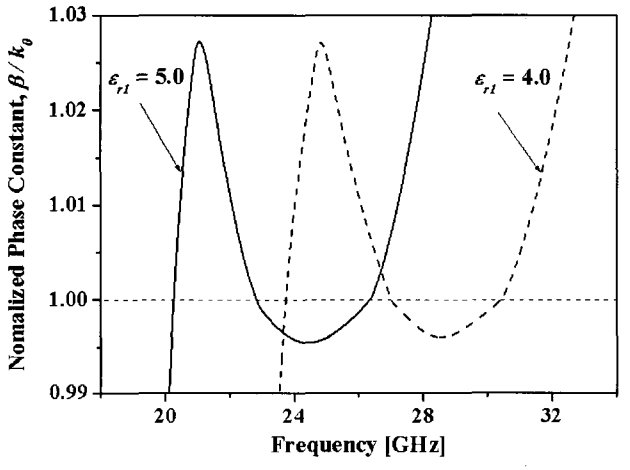

Fig. 8. Enlarged scale of normalized phase constants near unity for TM_{02} mode when radius of dielectric rod is 5.0 mm with different dielectric constants (ε_{r1}=5.0 and ε_{r1}=4.0).

Furthermore, with a small rod dielectric constant, the second antenna mode region of the TM_{01} mode was larger, whereas the spectral widths of the second antenna mode of the higher-order modes(TM_{02} mode) were smaller, as listed in Table 2(b).

V. Conclusion

The current study considered the leaky dispersion characteristics of a circular dielectric rod for several lower-order modes below the cutoff frequency of the guided mode. The dispersion characteristics were investigated based on precisely determined complex propagation constants using Davidenko's method. The effects of the dielectric constant and radius of the rod on the leaky dispersion characteristics were also examined. Several features of the leaky dispersion characteristics of a circular dielectric rod can be summarized as follows.

1. The TM_{01} mode does not have a reactive mode and spectral gap.
2. The higher-order modes have another antenna mode between the spectral gap and the guided mode.
3. The spectral gap is not always consistent with the transition region between the leaky and guided modes.
4. The spectral widths of the nonphysical mode region, reactive mode region, two antenna mode regions, and spectral gap region tend to increase with an increase in the order of the modes.
5. Except for the second antenna mode of the higher order modes, the spectral widths of each mode region tend to increase with a decrease in both the radius and the dielectric constant of the rod.

This work was supported by grant No. R01-2004-000-10158-0 from the Basic Research Program of the Korea Science & Engineering Foundation.

References

[1] E. Snitzer, "Cylindrical dielectric waveguide modes", *J. Opt. Soc. Am.*, vol. 51, no. 5, pp. 491-498, May 1961.

[2] F. Mesa, D. R. Jackson, "Investigation of integration paths in the spectral-domain analysis of leaky modes on printed circuit lines", *IEEE Trans. on Microwave Theory & Tech.*, vol. 50, no. 10, pp. 2267-2275, Oct. 2002.

[3] J. Arnbak, "Leaky waves on a dielectric rod", *Electronics Letters*, vol. 5, no. 3, pp. 41-42, Feb. 1969.

[4] H. A. N. Hejase, "On the use of Davidenko's method in complex root search", *IEEE Trans. on Microwave Theory & Tech.*, vol. 41, no. 1, pp. 141-143, Jan. 1993.

[5] K. Naishadham, L. B. Felsen, "Dispersion of waves guided along a cylindrical substrate-superstrate layered medium", *IEEE Trans. on Antennas & Prop.*, vol. 41, no. 3, pp. 304-313, Mar. 1993.

[6] K. Naishadham, H. W. Yao, "An efficient computation of transient scattering by a perfectly conducting cylinder", *IEEE Trans. on Antennas and Prop.*, vol. 41, no. 11, pp. 1509-1515, Nov. 1993.

[7] S. H. Talisa, "Application of Davidenko's method to the solution of dispersion relations in lossy waveguiding systems", *IEEE Trans. on Microwave Theory & Tech.*, vol. 33, no. 10, pp. 967-971, Oct. 1985.

[8] M. Shabat, "Numerical algorithms for modeling hybrid surface plasmon polaritons guided by metal

films", *Microwave & Opt. Tech. Lett.*, vol. 16, no. 2, pp. 122-124, Oct. 1997.

[9] M. M. Shabat, M. A. Abdel-Naby, Y. S. Madi, and D. Jäger, "Complex zeros of moving optical waveguides", *Microwave & Opt. Tech. Lett.*, vol. 21, no. 6, pp. 465-470, Jun. 1999.

[10] M. M. Shabat, D. Jäger, M. A. Abdel-Naby, and N. M. Barakat, "Numerical and analytical solutions of dispersion equation in lossy nonlinear waveguideing system", *Microwave & Opt. Tech. Lett.*, vol. 22, no. 4, pp. 273-278, Aug. 1999.

[11] S. D. Conte, C. Boor, *Elementary Numerical Analysis: An Algorithmic Approach*, Third Edition, McGraw-Hill Kogakusha, Ltd., 1980.

[12] J. A. Stratton, *Electromagnetic Theory*, McGraw-Hill Book Company, Inc., 1941.

[13] A. Ishimaru, *Electromagnetic Wave Propagation, Radiation, and Scattering*, Prentice Hall, Inc., 1991.

[14] D. G. Zill, M. R. Cullen, *Advanced Engineering Mathematics*, PWS Publishing Company, 1992.

[15] S. Wolfram, *The MATHEMATICA® Book*, 4th Ed., Cambridge University Press, 1999.

[16] P. Lampariello, F. Frezza, H. Shigesawa, M. Tsuji, and A. A. Oliner, "A versatile leaky-wave antenna based on stub-loaded rectangular waveguide: Part I - Theory", *IEEE Trans. on Antennas & Prop.*, vol. 46, no. 7, pp. 1032-1041, Jul. 1998.

[17] X. Y. Zeng, S. J. Xu, K. Wu, and K. M. Luk, "Properties of guided modes on open structures near the cutoff region using a new version of complex effective dielectric constant", *IEEE Trans. on Microwave Theory & Tech.*, vol. 50, no. 5, pp. 1417-1424, May 2002.

[18] P. Lampariello, F. Frezza, and A. A. Oliner, "The transition region between bound-wave and leaky-wave ranges for a partially dielectric-loaded open guiding structure", *IEEE Trans. Microwave Theory & Tech.*, vol. 38, no. 12, pp. 1831-1836, Dec. 1990.

Ki Young Kim

He received the B.S., M.S., and Ph.D. degrees all in electronic engineering from Kyungpook National University, Daegu, Korea, in 1998, 2001, and 2005, respectively. He was with the Pohang Accelerator Laboratory(PAL), where he developed photocathode RF gun. He is currently a postdoctoral fellow with Kyungpook National University. His recent research include guided and leaky waves in guided wave structures, surface plasmon polaritons in metals and metamaterials, surface waves in carbon nanotubes, subwavelength optics and its applications, and various equivalent circuit modeling. He was the recipient of the "2002 Best Paper Award" by the IEEE Seoul Section.

Heung-Sik Tae

He received the B.S. degree from the department of electrical engineering, Seoul National University, Seoul, Korea, in 1986 and his M.S. and Ph.D. degrees in plasma engineering from Seoul National University in 1988 and 1994, respectively. Since 1995, he has been employed as an Associate Professor in the school of electronic and electrical engineering, Kyungpook National University in Daegu, Korea. His research interests include the design of millimeter wave guiding structures, MEMS or thick-film processing for millimeter wave devices and the optical characterization and driving circuit of plasma display panels. Dr. Tae is a member of the IEEE.

Jeong-Hae Lee

He received his B.S. and M.S. degrees in electrical engineering in 1985 and 1988, respectively, from Seoul National University, Korea and his Ph.D. degree in electrical engineering in 1996 from the University of California, Los Angeles, USA. From 1993 to 1996, he was a Visiting Scientist of General Atomics, San Diego, USA, where his major research was to develop a millimeter wave diagnostic system and to study plasma wave physics. Since 1996, he has been at Hongik University, Seoul, Korea, where he is an Associate Professor in the department of radio science and communication engineering. His current research interests include microwave/millimeter wave circuits and measurements.